# KaVA Status Report for 2016B

KaVA User Support Team, NAOJ and KASI

April 18, 2016

# Contents

1	Inti	roduction	4											
2	Sys	System												
	2.1	Array	5											
	2.2	Antennas	6											
		2.2.1 Brief Summary of VERA Antennas	6											
		2.2.2 Brief Summary of KVN Antennas	6											
		2.2.3 Aperture Efficiency	7											
		2.2.4 Beam Pattern and Size	8											
	2.3													
		2.3.1 Brief Summary of VERA Receiving System	9											
		2.3.2 Brief Summary of KVN Receiving System	10											
	2.4	Digital Signal Process	14											
	2.5	Recorders	14											
	2.6	Correlators	15											
	2.7	Calibration	15											
		2.7.1 Delay and Bandpass Calibration	15											
		2.7.2 Gain Calibration	16											
	2.8	Geodetic Measurement	16											
		2.8.1 Brief Summary of VERA Geodetic Measurement	16											
		2.8.2 Brief Summary of KVN Geodetic Measurement	17											
3	Obs	serving Proposal	19											
	3.1	Call for Proposal (CfP)	19											
	3.2	Proposal Submission	19											
	3.3	Observation Mode	19											
	3.4	Target of Opportunity (ToO) observations												
	3.5	Angular Resolution and Largest Detectable Angular Scale 2												
	3.6	Sensitivity	20											
	3.7	Calibrator Information	22											
	3.8	Date Archive	23											
4	Obs	servation and Data Reduction	24											
	4.1	Preparation	24											
	4.2	Observation and Correlation	24											
	4.3	Data Reduction	24											
	4.4	Further Information	25											

$\mathbf{A}$	New	observation mode from 2016B	26
	A.1	Fast antenna nodding mode	26
	A.2	1-beam hybrid (K/Q/W) mode	26

### 1 Introduction

This document summarizes the current observational capabilities of KaVA (KVN and VERA Array), which is a combined VLBI network of KVN (Korean VLBI Network) and VERA (VLBI Exploration of Radio Astrometry) operated by Korea Astronomy and Space Science Institute (KASI) and National Astronomical Observatory of Japan (NAOJ), respectively (see Figure 1). In 2016, KaVA system is still being developed and some capabilities are remained to be implemented.

KaVA invites proposals for common use observations to be carried out from 15th June 15 2016 to 15th January 2017 (2016B). The maximum observing time per proposal is 48 hours. If requested in the proposals, the observation time can be allocated over a year, until 15th June, 2017, for this call. But the maximum observation time will be NOT increased. Two new observation modes are available from this call, Fast antenna nodding mode and 1-beam hybrid (KVN multi-freuquency support) mode. This call for proposals (CfP) is offered for open use in a shared-risk mode.

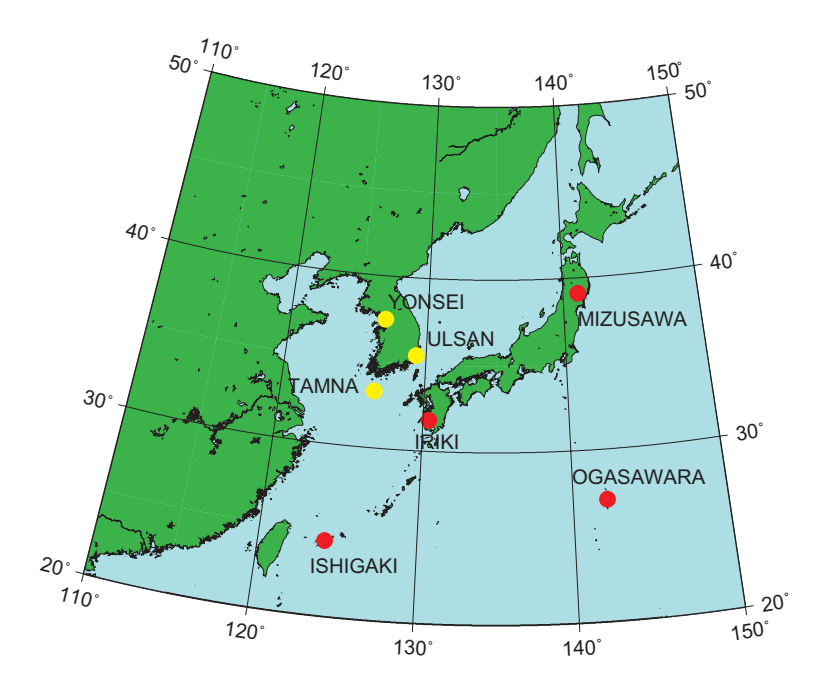


Figure 1: Array configuration of KaVA.

VERA is a Japanese VLBI array to explore the 3-dimensional structure of the Milky Way Galaxy based on high-precision astrometry of Galactic maser sources. VERA array consists of four 20 m radio telescopes located at Mizusawa, Iriki, Ogasawara, and Ishigakijima with baseline ranges from 1000 km to 2300 km. The construction of VERA array was completed in 2002, and it is under regular operation since the fall of 2003. VERA was opened to international users in the K band (22 GHz) and Q band (43 GHz) from 2009. Most unique aspect of VERA is "dual-beam" telescope, which can simultaneously observe nearby two sources. While single-beam VLBI significantly suffers from fluctuation of atmosphere, dual-beam observations with VERA effectively cancel out the atmospheric fluctuations, and then VERA can measure relative positions of target sources to reference sources with higher accuracy based on the 'phase-referencing' technique. For more detail, visit the following web site:

#### http://veraserver.mtk.nao.ac.jp/index.html.

KVN is the mm-wavelength VLBI facility in Korea. It consists of three 21 m radio telescopes, which are located in Seoul (Yonsei University), Ulsan (University of Ulsan), and Jeju island (ex-Tamna University), and produces an effective spatial resolution equivalent to that of a 500 km radio telescope. KASI has developed innovative multifrequency band receiver systems, observing four different frequencies at 22, 43, 86, and 129 GHz simultaneously. With this capability, KVN will provide opportunities to study the formation and death processes of stars, the structure and dynamics of our own Galaxy, the nature of Active Galactic Nuclei and so on at milli-arcsecond (mas) resolutions. For more detail, visit the following web site and paper (Lee et al. 2011):

#### http://kvn.kasi.re.kr/eng.

KaVA was formed in 2010, on the basis of the VLBI collaboration agreement between KASI and NAOJ. KaVA complements baseline length range up to 2270 km, and can achieve a good imaging quality. Currently, KaVA supports observations at K band and Q band in left-hand-circular polarization with a data aggregation rate of 1024 Mega bit per seconds (bps) (=1 Gbps). This document is intended to give astronomers necessary information for proposing observations with KaVA. For more detail, visit the following web site:

#### http://kava.kasi.re.kr.

In 2014, the first results from KaVA have been published. Matsumoto et al. (2014) report the first VLBI detection of the 44 GHz methanol maser emission associated with a massive star-forming region. They demonstrate the unique capability of KaVA to image extended maser features. Niinuma et al. (2014) report the detailed analysis of KaVA observations of active galactic nuclei (AGN). The paper discuss about imaging quality and flux calibration accuracy of KaVA. These two papers are useful to know basic properties of KaVA.

# 2 System

# 2.1 Array

KaVA consists of 7 antenna sites in VERA-Mizusawa, VERA-Iriki, VERA-Ogasawara, VERA-Ishigakijima, KVN-Yonsei, KVN-Ulsan and KVN-Tamna with 21 baselines (see Figure 1). The maximum baseline length is 2270 km between Mizusawa and Ishigakijima, and the minimum baseline length is 305 km between Yonsei and Ulsan. The maximum angular resolution expected from the baseline length is about 1.2 mas for K band and about 0.6 mas for Q band. The geographic locations and coordinate of each KaVA antenna in the coordinate system of epoch 2009.0 are summarized in Table 1. The geographic locations and coordinate of each KaVA antenna are summarized in Table 1. Figure 2 shows examples of uv plane coverage.

The averaged velocities of VERA sites in Table 2 are predicted value at the epoch of January 01, 2015. Reference frame of these coordinates is ITRF2008. The rates of the coordinates of Mizusawa, Iriki, Ogasawara and Ishigakijima are the average value of change of the coordinates from January 01, 2014 to December 31, 2014. The 2011 off the Pacific coast of Tohoku Earthquake (Mj=9.0) brought the co-seismic large step and non-linear post-seismic movement to the coordinates of Mizusawa. Co-seismic steps of

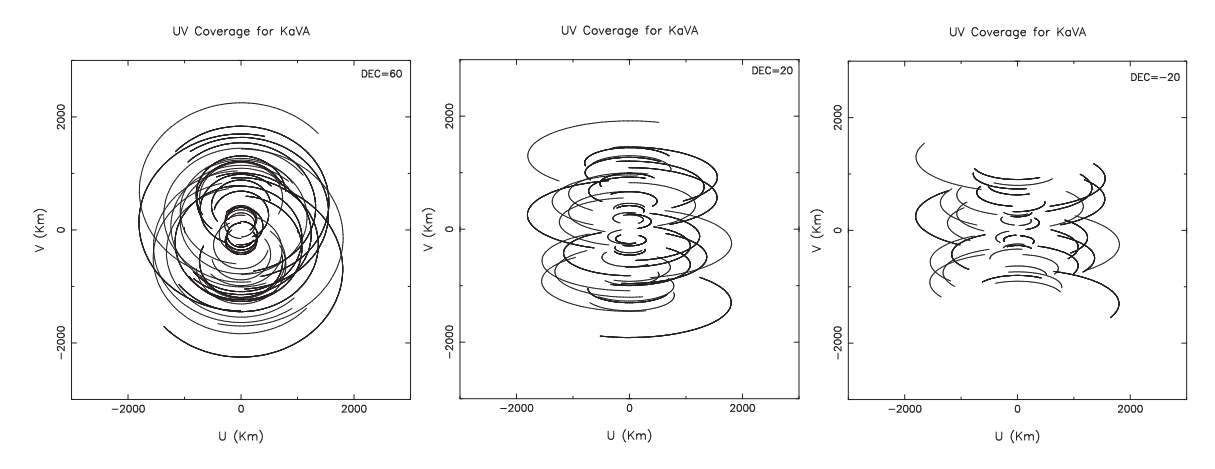


Figure 2: The uv plane coverage ( $\pm 3000$  km) expected with KaVA antennas from an observation over elevation of  $20^{\circ}$ . Each panel shows the uv coverage for the declination of  $60^{\circ}$  (left),  $20^{\circ}$  (center), and  $-20^{\circ}$  (right).

the coordinates of Mizusawa are dX=-2.0297m, dY=-1.4111m and dZ=-1.0758m. The creeping continues still now, though decreased. The changes of coordinates by the post-seismic creeping are dX=-0.8574m, dY=-0.5387m and dZ=-0.2398m in total from March, 12, 2011 to Jan, 01, 2015.

In the case of KVN, all antenna locations are measured with GPS system. The antenna positions of KVN are regularly monitored both with GPS system and geodetic VLBI observations in collaboration with VERA. No velocity information is available for KVN stations.

### 2.2 Antennas

#### 2.2.1 Brief Summary of VERA Antennas

All the telescopes of VERA have the same design, being a Cassegrain-type antenna on AZ-EL mount. Each telescope has a 20 m diameter dish with a focal length of 6 m, with a sub-reflector of 2.6 m diameter. The dual-beam receiver systems are installed at the Cassegrain focus. Two receivers are set up on the Stewart-mount platforms, which are sustained by steerable six arms, and with such systems one can simultaneously observe two adjacent objects with a separation angle between 0.32 and 2.2 deg. The whole receiver systems are set up on the field rotator (FR), and the FR rotate to track the apparent motion of objects due to the earth rotation. Table 3 summarizes the ranges of elevation (EL), azimuth (AZ) and field rotator angle (FR) with their driving speeds and accelerations. In the case of single beam observing mode, one of two beams is placed at the antenna vertex (separation offset of 0 deg).

#### 2.2.2 Brief Summary of KVN Antennas

The KVN antennas are also designed to be a shaped-Cassegrain-type antenna with an AZ-EL mount. The telescope has a 21 m diameter main reflector with a focal length of 6.78 m. The main reflector consists of 200 aluminum panels with a manufacturing surface accuracy of about 65  $\mu$ m. The slewing speed of the main reflector is 3 °/sec, which enables fast position-switching observations (Table 3). The sub-reflector position, tilt,

Table 1: Geographic locations and motions of each KaVA antenna.

	East	North	Ellipsoidal			
	Longitude	Latitude	Height	$X^a$	$Y^a$	$\mathrm{Z}^a$
Site	[° ′ ′′]	[° ′ ′′]	[m]	[m]	[m]	[m]
Mizusawa	141 07 57.3	39 08 00.7	116.4	-3857244.6425	3108782.9988	4003899.1960
Iriki	$130\ 26\ 23.6$	$31\ 44\ 52.4$	573.6	-3521719.8241	4132174.6271	3336994.1240
Ogasawara	$142\ 12\ 59.8$	$27\ 05\ 30.5$	273.1	-4491068.5536	3481545.0831	2887399.7333
Ishigakijima	$124\ 10\ 15.6$	$24\ 24\ 43.8$	65.1	-3263995.1565	4808056.3118	2619948.7878
$Yonsei^b$	$126\ 56\ 27.4$	$37\ 33\ 54.9$	139	-3042280.9035	4045902.6564	3867374.3087
$Ulsan^b$	$129\ 14\ 59.3$	$35\ 32\ 44.2$	170	-3287268.5430	4023450.1448	3687379.9675
$\mathrm{Tamna}^b$	$126\ 27\ 34.4$	$33\ 17\ 20.9$	452	-3171731.5532	4292678.5258	3481038.7679

<sup>&</sup>lt;sup>a</sup>The epoch of the coordinates of VERA is January, 01, 2015.

Table 2: Station code and average velocity of each VERA antenna.

				J		
Site	$IVS2^a$	$IVS8^b$	$\mathrm{CDP}^c$	$\Delta X [m/yr]^d$	$\Delta Y [m/yr]^d$	$\Delta Z [m/yr]^d$
Mizusawa	Vm	VERAMZSW	7362	-0.0887	-0.0489	-0.0047
Iriki	Vr	VERAIRIK	7364	-0.0210	-0.0088	-0.0151
Ogasawara	Vo	VERAOGSW	7363	0.0266	0.0275	0.0084
Ishigakijima	$V_{\rm S}$	VERAISGK	7365	-0.0393	0.0004	-0.0486

<sup>&</sup>lt;sup>a</sup>IVS 2-characters code

and tip are remotely controlled and modeled to compensate for the gravitational deformation of the main reflector and for the sagging-down of the sub-reflector itself.

Table 3: Driving performance of KaVA antennas.

Driving axis	Driving range	Max. driving speed	Max. driving acceleration
		VERA	
$\overline{\mathrm{AZ}^a}$	$-90^{\circ} \sim 450^{\circ}$	$2.1^{\circ}/\mathrm{sec}$	$2.1^{\circ}/\mathrm{sec}^2$
$\operatorname{EL}$	$5^{\circ} \sim 85^{\circ}$	$2.1^{\circ}/\mathrm{sec}$	$2.1^{\circ}/\mathrm{sec}^2$
$FR^b$	$-270^{\circ} \sim 270^{\circ}$	$3.1^{\circ}/\mathrm{sec}$	$3.1^{\circ}/\mathrm{sec}^2$
		KVN	
$\mathrm{AZ}^a$	$-90^{\circ} \sim 450^{\circ}$	$3^{\circ}/\mathrm{sec}$	$3^{\circ}/\mathrm{sec}^2$
EL	$5^{\circ} \sim 85^{\circ}$	$3^{\circ}/\mathrm{sec}$	$3^{\circ}/\mathrm{sec}^2$

<sup>&</sup>lt;sup>a</sup>The north is  $0^{\circ}$  and the east is  $90^{\circ}$ .

#### 2.2.3 Aperture Efficiency

The aperture efficiency of each VERA antenna is about 40–50% in both K band and Q band (see Table 4 for the 2014 and 2012 data for VERA and KVN, respectively). These values will be measured and updated in 2015-2016 winter season. These measurements were based on the observations of Jupiter assuming that the brightness temperature of Jupiter is 160 K in both the K band and the Q band. Due to the bad weather condition in some of the sessions, the measured efficiencies show large scatter.

<sup>&</sup>lt;sup>b</sup>The KVN antenna positions are obtained by the KaVA K-band geodesy program on January 24, 2014.

 $<sup>^</sup>b {
m IVS}$  8-characters code

<sup>&</sup>lt;sup>c</sup>CDP (NASA Crustal Dynamics Project) code

<sup>&</sup>lt;sup>d</sup>The epoch of the coordinates is January 01, 2015. Average speed was obtained from the VLBI data from January 01, 2014 to January 01, 2015.

<sup>&</sup>lt;sup>b</sup>FR is 0° when Beam-1 is at the sky side and Beam-2 is at the ground side, and CW is positive when an antenna is seen from a target source.

	Table 4: A	perture efficienc	v and beam	size of KaVA	antennas.
--	------------	-------------------	------------	--------------	-----------

	K bar	nd (22 GHz)	Q ban	d (43 GHz)
	$\overline{\eta_{ m A}}$	HPBW	$\overline{\eta_{ m A}}$	HPBW
Antenna Name	(%) (arcsec)		(%)	(arcsec)
Mizusawa	48	143	46	76
Iriki	46	140	41	76
Ogasawara	46	155	40	75
Ishigakijima	47	144	44	75
Yonsei	55	127	63	63
Ulsan	63	124	61	63
Tamna	60	126	63	63

However, we conclude that the aperture efficiencies are not significantly changed compared with previous measurements. The elevation dependence of aperture efficiency for VERA antenna was also measured from the observation toward maser sources. Figures 3 shows the relations between the elevation and the aperture efficiency measured for VERA Iriki station. The gain curves are measured by observing the total power spectra of intense maser sources. The aperture efficiency in low elevation of  $\leq 20$  deg decreases slightly, but this decrease is less than about 10%. Concerning this elevation dependence, the observing data FITS file include a gain curve table (GC table), which is AIPS readable, in order to calibrate the dependence when the data reduction.

The aperture efficiency and beam size for each KVN antenna are also listed in Table 4. Aperture efficiency of KVN varies with elevation as shown in Figure 3. The main reflector panels of KVN antennas were installed to give the maximum gain at the elevation angle of 48°. The sagging of sub-reflector and the deformation of main reflector by gravity with elevation results in degradation of antenna aperture efficiency with elevation. In order to compensate this effect, KVN antennas use a hexapod to adjust sub-reflector position. Figure 3 shows the elevation dependence of antenna aperture efficiency of the KVN 21 m radio telescopes measured by observing Venus or Jupiter. By fitting a second order polynomial to the data and normalizing the fitted function with its maximum, we derived a normalized gain curve which has the following form:

$$G_{\text{norm}} = A_0 E L^2 + A_1 E L + A_2,$$
 (1)

where EL is the elevation in degree.

#### 2.2.4 Beam Pattern and Size

Figure 4 show the beam patterns in the K band. The side-lobe level is less than about -15 dB, except for the relatively high side-lobe level of about -10 dB for the separation angle of 2.0 deg at Ogasawara station. The side-lobe of the beam patterns has an asymmetric shape, but the main beam has a symmetric Gaussian shape without dependence on separation angle. The measured beam sizes (HPBW) in the K band and the Q band based on the data of the pointing calibration are also summarized in Table 4. The main beam sizes show no dependence on the dual-beam separation angle.

The optics of KVN antenna is a shaped Cassegrain type of which the main reflector and subreflector are shaped to have a uniform illumination pattern on an aperture plane. Because of the uniform illumination, KVN antennas can get higher aperture efficiency than value of typical Cassegrain type antenna. However, higher side-lobe level

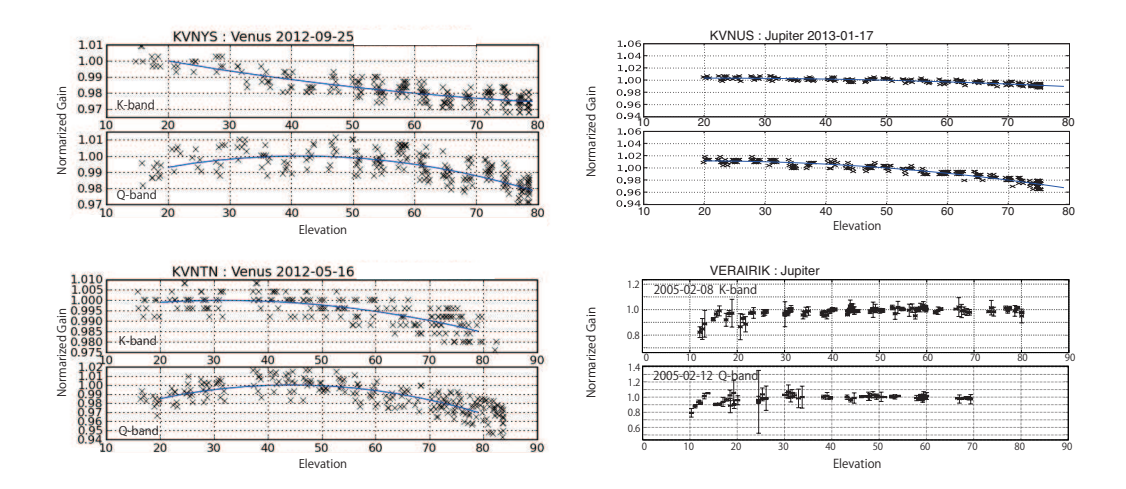


Figure 3: The elevation dependence of the aperture efficiency for KVN three antennas and VERA Iriki antenna. For KVN antennas, the maximum gain is given at the elevation angle of 48°. The efficiency in K-band (on Feb 8, 2005) and the Q-band (on Feb 12, 2005) for VERA Iriki antenna is shown in *bottom right*. The efficiency is relative value to the measurement at  $EL = 50^{\circ}$ .

is inevitable. OTF images of Jupiter at K and Q bands are shown in Figure 4. The map size is  $12'\times10'$  and the first side-lobe pattern is clearly visible. Typical side-lobe levels of KVN antennas are 13-14dB.

#### 2.3 Receivers

#### 2.3.1 Brief Summary of VERA Receiving System

Each VERA antenna has the receivers for 4 bands, which are S (2 GHz), C (6.7 GHz), X (8 GHz), K (22 GHz), and Q (43 GHz) bands. For the common use in 2009, the K band and the Q band are open for observing. The low-noise HEMT amplifiers in the K and Q bands are enclosed in the cryogenic dewar, which is cooled down to 20 K, to reduce the thermal noise. The range of observable frequency and the typical receiver noise temperature  $(T_{\rm RX})$  at each band are summarized in the Table 5 and Figure 5.

Table 5: Frequency range and  $T_{RX}$  of VERA and KVN receivers.

	Frequency Range	$T_{\rm RX}{}^a$	
Band	[GHz]	[K]	Polarization
		VERA	
K	21.5-23.8	30-50	LCP
Q	42.5 - 44.5	70-90	LCP
		KVN	
K	21.25 - 23.25	30-40	LCP/RCP
Q	42.11-44.11	70-80	LCP/RCP
		(40-50  for Ulsan)	

<sup>&</sup>lt;sup>a</sup>Receiver noise temperature

After the radio frequency (RF) signals from astronomical objects are amplified by the receivers, the RF signals are mixed with standard frequency signal generated in

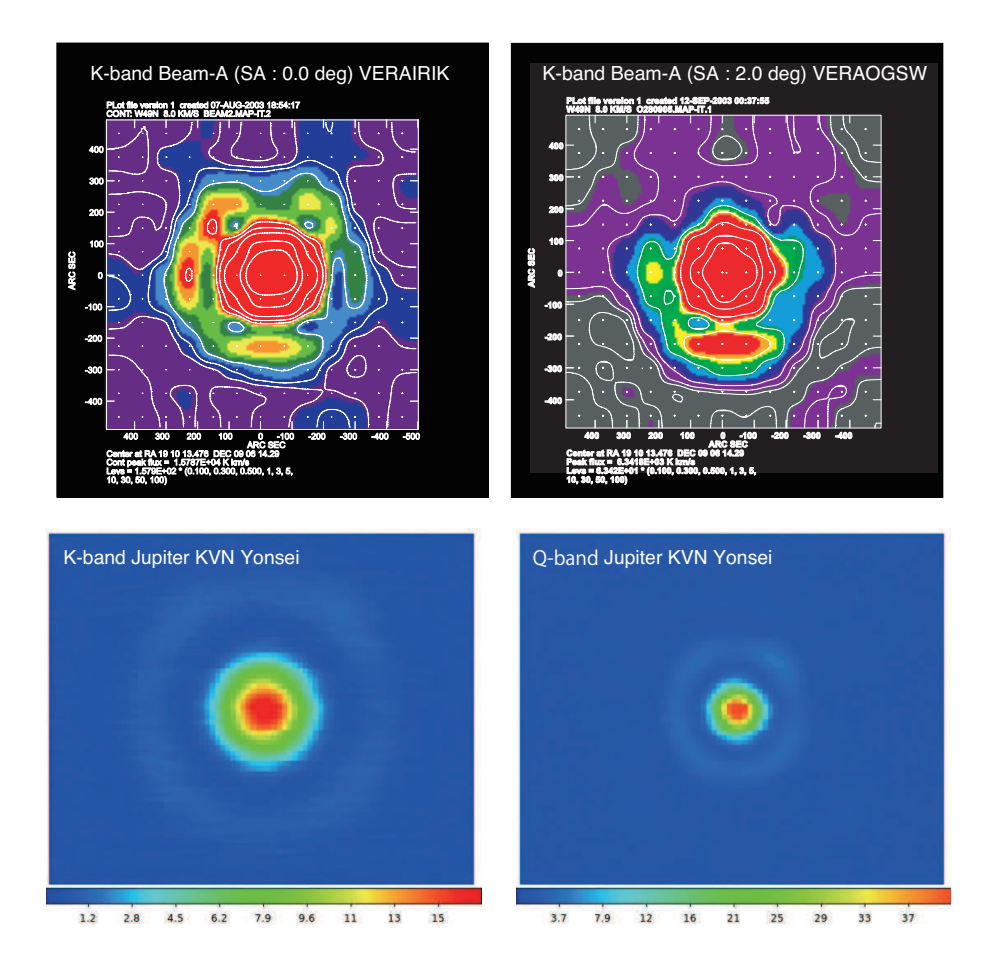


Figure 4: The beam patterns in the K-band for VERA (A-beam) Iriki with the separation angle of  $0^{\circ}$  (*Upper left*) and Ogasawara with the separation angle of  $2.0^{\circ}$  (*Upper right*), and in K/Q-band for KVN Yonsei. The patterns of VERA antennas were derived from the mapping observation of strong H<sub>2</sub>O maser toward W49N, which can be assumed as a point source, with grid spacing of 75". In the case of KVN antennas, the patterns were derived from the OTF images of Venus at K/Q-band.

the first local oscillator to down-convert the RF to an intermediate frequency (IF) of 4.7 GHz–7 GHz. The first local frequencies are fixed at 16.8 GHz in the K band and at 37.5 GHz in the Q band. The IF signals are then mixed down again to the base band frequency of 0–512 MHz. The frequency of second local oscillator is tunable with a possible frequency range between 4 GHz and 7 GHz. The correction of the Doppler effect due to the earth rotation is carried out in the correlation process after the observation. Therefore, basically the second local oscillator frequency is kept to be constant during the observation. Figure 6 shows a flow diagram of these signals for VERA.

#### 2.3.2 Brief Summary of KVN Receiving System

The KVN quasi-optics are uniquely designed to observe 22, 43, 86 and 129 GHz band simultaneously (Han et al. 2008, 2013). Figure 7 shows the layout of quasi-optics and receivers viewing from sub-reflector side. The quasi-optics system splits one signal from sub-reflector into four using three dichroic low-pass filters marked as LPF1, LPF2 and

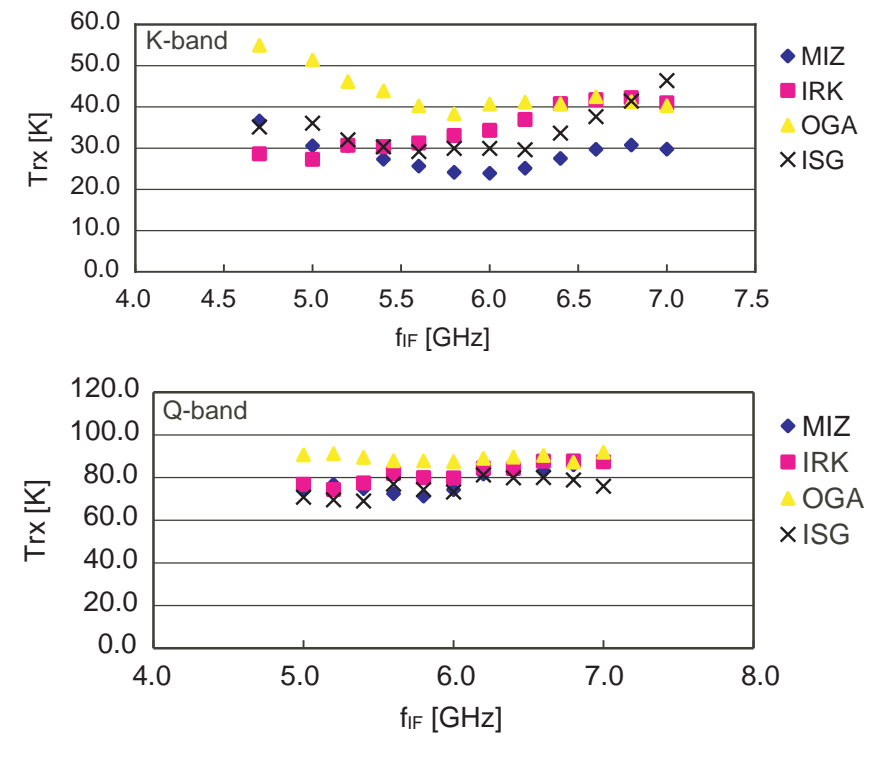


Figure 5: Receiver noise temperature for each VERA antenna. Top and bottom panels show measurements in the K and Q bands, respectively. Horizontal axis indicate an IF (intermediate frequency) at which  $T_{\rm RX}$  is measured. To convert it to RF (radio frequency), add 16.8 GHz in the K band and 37.5 GHz in the Q band to the IF frequency.

LPF3 in the Figure 7. The split signals into four different frequency bands are guided to corresponding receivers.

Figures 8 shows a signal flows in KVN system. The 22, 43 and 86 GHz band receivers are cooled HEMT receivers and the 129 GHz band receiver is a SIS mixer receiver. All receivers receive dual-circular-polarization signals. Among eight signals (four dual-polarization signals), four signals selected by the IF selector are down-converted to the input frequency band of the sampler. The instantaneous bandwidth of the 1st IF of each receiver is limited to 2 GHz by the band-pass filter. The 1st IF signal is down-converted by BBCs to the sampler input frequency (512-1024 MHz) band.

Typical noise temperatures of K and Q bands are presented in Table 5. Since the calibration chopper is located before the quasi-optics as shown in Figure 7, the loss of quasi-optics contributes to receiver noise temperature instead of degrading antenna aperture efficiency. Therefore, the noise temperature in the table includes the contribution due to the quasi-optics losses.

The receiver noise temperatures of three stations are similar to each other except that the noise temperature of the Ulsan 43 GHz because of the different type of thermal isolator, which is used to reduce heat flow from the feed horn in room temperature stage to cryogenic cooled stage more effectively.

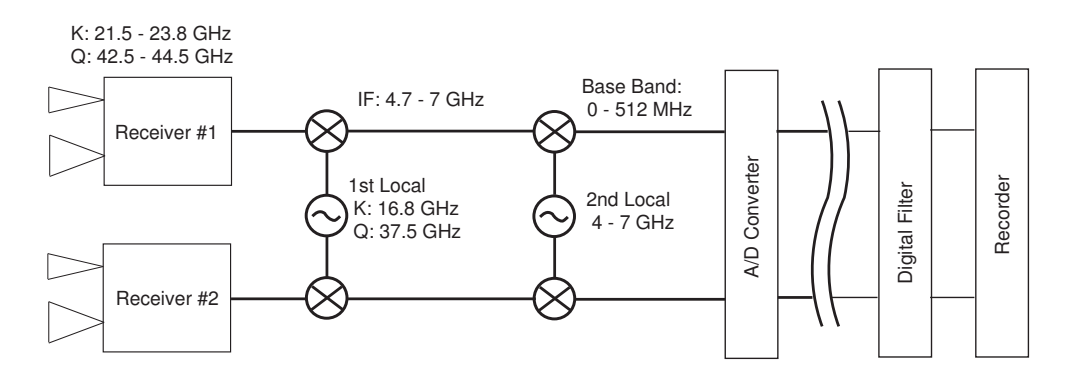


Figure 6: Flow diagram of signals from receiver to recorder for VERA.

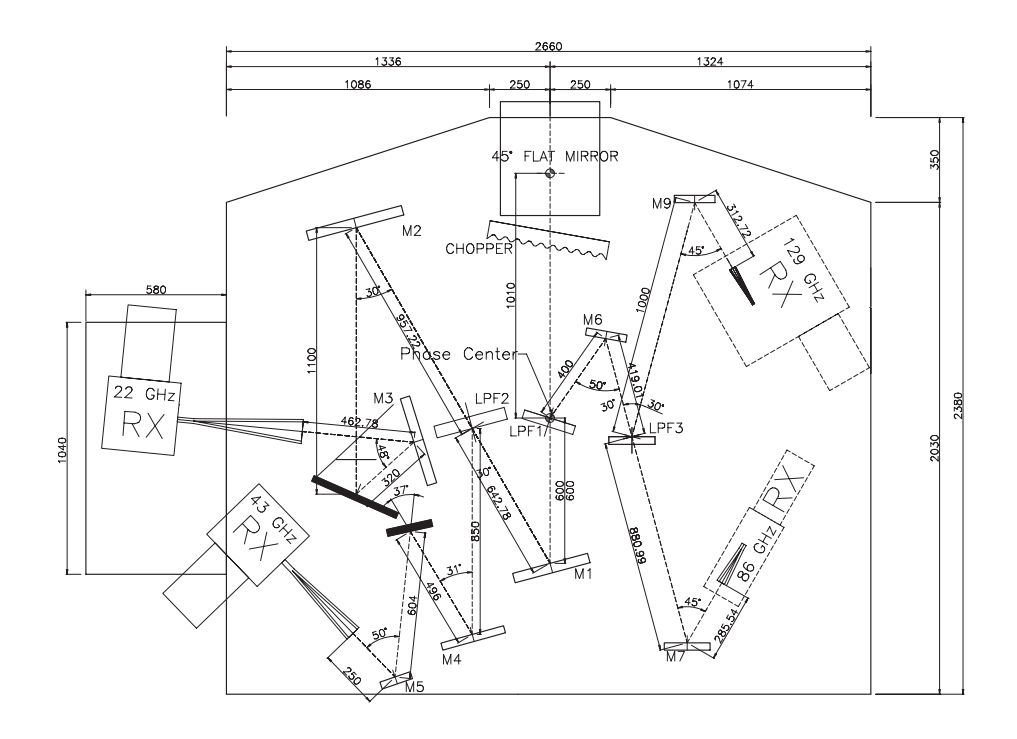


Figure 7: KVN multi-frequency receiving system (Han et al. 2008, 2013).

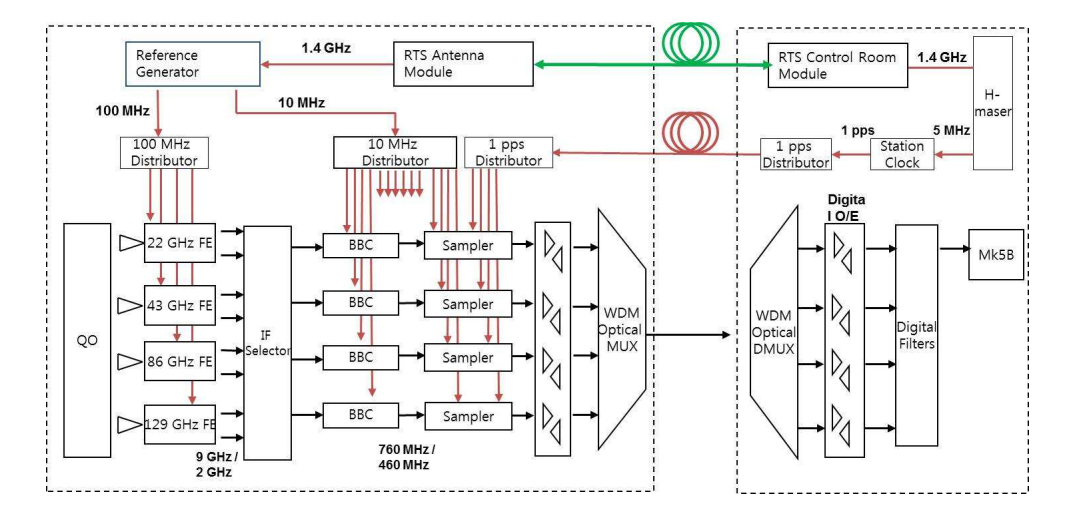


Figure 8: Flow diagram of signals from receiver to recorder for KVN (Oh et al. 2011).

Table 6: Digital filter mode for KaVA.

Mode	Rate	Num.	$BW/CH^b$		Freq. range <sup><math>d</math></sup>	Side	
Name	(Mbps)	$\mathrm{CH}^a$	(MHz)	$\mathrm{CH}^c$	(MHz)	$\mathrm{Band}^e$	$\mathrm{Note}^f$
GEO1K*	1024	16	16	1	0 - 16	U	
				2	32 - 48	U	
				3	64 - 80	U	
				4	96 - 112	U	
				5	128 - 144	U	
				6	160 - 176	U	
				7	192 - 208	U	
				8	224 - 240	U	
				9	256 - 272	U	Target line (e.g. $H_2O$ )
				10	288 - 304	U	
				11	320 - 336	U	
				12	352 - 368	U	
				13	384 - 400	U	
				14	416 - 432	U	
				15	448 - 464	U	
				16	480 - 496	Ü	
GEO1S*	1024	16	16	1	112 - 128	L	
GLOIS	1021	10	10	2	128 - 144	U	
				3	144 - 160	Ĺ	
				4	160 - 176	U	
				5	176 - 192	L	
				6	192 - 208	U	
				7	208 - 224	L	
				8	224 - 240	U	
				9	240 - 256	L	T
				10	256 - 272	U	Target line (e.g. $H_2O$ )
				11	272 - 288	L	
				12	288 - 304	U	
				13	304 - 320	L	
				14	320 - 336	U	
				15	336 - 352	${ m L}$	
				16	352 - 368	U	
VERA7SIOS*	1024	16	16	1	32 - 48	U	
				2	64 - 80	U	
				3	80 - 96	${ m L}$	SiO $(J=1-0, v=2)$
				4	96 - 112	U	
				5	128 - 144	U	
				6	160 - 176	U	
				7	192 - 208	U	
				8	224 - 240	U	
				9	256 - 272	U	
				10	288 - 304	U	
				11	384 - 400	Ŭ	SiO $(J=1-0, v=1)$
				12	320 - 336	Ü	- ( /
				13	352 - 368	Ü	
				14	416 - 432	U	
				15	448 - 464	U	
				16	480 - 496	U	
* 4 11 1 1	C A D	/3.77			ERA/KVN). Mo		

<sup>\*</sup>All channels are for A-Beam (VERA) and LCP (VERA/KVN). Mode names are tentative.

 $<sup>^</sup>a$ Total number of channels

 $<sup>{}^</sup>b\mathrm{Bandwidth}$  per channel in MHz

<sup>&</sup>lt;sup>c</sup>Channel number

 $<sup>^</sup>d\mathrm{Filtered}$  frequency range in the base band (MHz)

<sup>&</sup>lt;sup>e</sup>Side Band (LSB/USB)

fExample of spectral line setting

Table 7:	New	digital	filter	mode	for	KaVA.

Mode	Rate	Num.	$BW/CH^b$		Freq. range <sup><math>d</math></sup>	Side	
Name	(Mbps)	$\mathrm{CH}^a$	(MHz)	$\mathrm{CH}^c$	(MHz)	$\mathrm{Band}^e$	$Note^f$
VERA4S*	1024	8	32	1	128 - 160	U	
				2	160 - 192	L	
				3	192 - 224	U	
				4	224 - 256	L	
				5	256 - 288	U	
				6	288 - 320	L	
				7	320 - 352	U	
				8	352 - 384	${ m L}$	

<sup>\*</sup>All channels are for A-Beam (VERA) and LCP (VERA/KVN).

### 2.4 Digital Signal Process

In VERA system, A/D (analog-digital) samplers convert the analog base band outputs of 0–512 MHz  $\times 2$  beams to digital form. The A/D converters carry out the digitization of 2-bit sampling with the bandwidth of 512 MHz and the data rate is 2048 Mbps for each beam.

In KVN system, A/D samplers digitize signals into 2-bit data streams with four quantization levels. The base band output is 512–1024 MHz. The sampling rate is 1024 Mega sample per second (Msps) with 2-bit sampling resulting a 2048 Mbps=2 Gbps data rate at 512 MHz frequency bandwidth. Four streams of 512 MHz band width (2 Gbps data rate) can be obtained in the KVN multi-frequency receiving system simultaneously, which means that the total rate is 8 Gbps.

Since the total data recording rate is limited to 1024 Mbps (see the next section), only part of the sampled data can be recorded onto hard disks. The data rate reduction is done by digital filter system, with which one can flexibly choose number and width of recording frequency bands. Observers can select modes of the digital filter listed in the Table 6. For the 2016B KaVA observing season, four digital filter modes are available. From the 2016A season, a new digital filter mode called VERA4S is also available (Table 7). In VERA7SIOS mode in the Table 6, two transitions (v=1 & 2) of SiO maser in the Q band can be simultaneously recorded.

#### 2.5 Recorders

The KaVA observations are basically limited to record with 1024 Mbps data rate. To response 1 Gbps recording, VERA and KVN have OCTADISK and Mark5B recording systems, respectively. OCTADISK and Mark5B are hard disk recording systems developed at NAOJ and Haystack observatory, respectively. A high-speed magnetic tape recorder, DIR-2000, is no longer used. Their total bandwidths are 256 MHz because of 2-bit sampling.

<sup>&</sup>lt;sup>a</sup>Total number of channels

<sup>&</sup>lt;sup>b</sup>Bandwidth per channel in MHz

 $<sup>^</sup>c$ Channel number

<sup>&</sup>lt;sup>d</sup>Filtered frequency range in the base band (MHz)

<sup>&</sup>lt;sup>e</sup>Side Band (LSB/USB)

#### 2.6 Correlators

The correlation process is carried out by a VLBI correlator located at KJCC (Korea-Japan Correlation Center) at Daejeon, which has been developed as the KJJVC (Korea-Japan Joint VLBI Correlator) located at KJCC (Korea-Japan Correlation Center) project. Hereafter it is tentatively called "Daejeon correlator". The Daejeon correlator can process the data stream of up to 8192 Mbps from maximum 16 antenna stations at once. Currently the raw observed data of KVN stations are recorded and playbacked with Mark5B, and those of VERA stations are recorded and playbacked with OC-TADISK at the data rate of 1024 Mbps. Data formats available in the next observing season are 16 IFs×16 MHz ("C5 mode" in The Daejeon correlator terminology) and 8 IFs×32 MHz ("C4 mode"). The C4 mode is newly available from the 2016A season. Minimum integration times (time resolution) are 0.8192 seconds and 1.6384 seconds for C4 and C5 modes, respectively, and the number of frequency channels within each IF is 8192 for both modes (i.e. maximum frequency resolution is about 1.95 kHz). By default, the number of frequency channels is reduced to 128 (for continuum) or 512 (for line) via channel integration after correlation. One may put a special request of number of frequency channels to take better frequency resolution. The number of frequency channels can be selected among 512, 1024, 2048, 4096 or 8192. Final correlated data is served as FITS-IDI file.

Specification of The Daejeon correlator is summarized in Table 8.

Table 8: Specification of The Daejeon correlator<sup>a</sup>.

Max. number of antennas	16
correlation mode	C4(32 MHz Bandwidth, 8 stream)
	C5(16 MHz Bandwidth, 16 stream)
Max. number of corr./input	120  cross + 16  auto
Sub-array	$2 \operatorname{case}(12+4, 8+8)$
Bandwidth	512 MHz
Max. data rate/antenna	2048 Mbps VSI-H(32 parallels, 64MHz clock)
Max. delay compensation	$\pm$ 36,000 km
Max. fringe tracking	$1.075~\mathrm{kHz}$
FFT work length	16+16 bits fixed point for real, imaginary
Integration time	$25.6~\mathrm{msec} \sim 10.24~\mathrm{sec}$
Data output channels	8192 channels
Data output rate	Max. 1.4GB/sec at 25.6msec integration time
an 1 + 11	

<sup>&</sup>lt;sup>a</sup>For more details, see

http://kvn.kasi.re.kr/status\_report/correlator\_status.html.

#### 2.7 Calibration

Here we briefly summarize the calibration procedure of the KaVA data. Basically, most of the post-processing calibrations are done by using the AIPS (Astronomical Image Processing System) software package developed by NRAO (National Radio Astronomical Observatory).

#### 2.7.1 Delay and Bandpass Calibration

The time synchronization for each antenna is kept within 0.1  $\mu$ sec using GPS and high stability frequency standard provided by the hydrogen maser. To correct for

clock parameter offsets with better accuracy, bright continuum sources with accurately-known positions should be observed at usually every 60–80 minutes during observations. A recommended scan length for calibrators is 5–10 minutes. This can be done by the AIPS task FRING. The calibration of frequency characteristic (bandpass calibration) can be also done based on the observation of bright continuum source. This can be done by the AIPS task BPASS.

#### 2.7.2 Gain Calibration

Both VERA and KVN antennas have the chopper wheel of the hot load (black body at the room temperature), and the system noise temperature can be obtained by measuring the ratio of the sky power to the hot load power (so-called R-Sky method). Thus, the measured system noise temperature is a sum of the receiver noise temperature, spillover temperature, and contribution of the atmosphere (i.e. so-called  $T_{sys}^*$  corrected for atmospheric opacity). The hot load measurement can be made before/after any scan. Also, the sky power is continuously monitored during scans, so that one can trace the variation of the system noise temperature. The system noise temperature value can be converted to SEFD (System Equivalent Flux Density) by dividing by the antenna gain in K/Jy, which is derived from the aperture efficiency and diameter of each antenna. For the correlated data from KJCC,  $T_{sys}^*$  data (TY table) and antenna gain information (GC table) are provided with the ANTAB-readable format. KJCC makes complete version of ANTAB-readable file and provide it to PI. User support team supports PIs as appropriate. The TY and GC tables can be loaded by the AIPS task ANTAB, and these tables are converted to the SN table by the AIPS task APCAL.

Alternatively, one can calibrate the visibility amplitude by the template spectrum method, in which auto-correlation spectra of a maser source is used as the flux calibrator. This calibration procedure is made by the AIPS task ACFIT (see AIPS HELP for ACFIT for more detail).

Further correction is made for VLBI observations taken with 2-bit (4-level) sampling, for the systematic effects of non-optimal setting of the quantizer voltage thresholds. This is done by the AIPS task ACCOR. The amplitude calibrations with KaVA are accurate to 15% or better at K and Q bands.

#### 2.8 Geodetic Measurement

#### 2.8.1 Brief Summary of VERA Geodetic Measurement

Geodetic observations are performed as part of the VERA project observations to derive accurate antenna coordinates. The geodetic VLBI observations for VERA are carried out in the S/X bands and also in the K band. The S/X bands are used in the domestic experiments with the Geographical Survey Institute of Japan and the international experiments called IVS-T2. On the other hand, the K band is used in the VERA internal experiments. We obtain higher accuracy results in the K band compared with the S/X bands. The most up-to-date geodetic parameters are derived through geodetic analyses.

Non-linear post seismic movement of Mizusawa after the 2011 off the Pacific coast of Tohoku Earthquake continues. The position and velocity of Mizusawa is continuously

monitored by GPS. The coordinates in the Table 1 are provisional and will be revised with accumulation of geodetic data by GPS and VLBI.

In order to maintain the antenna position accuracy, the VERA project has three kinds of geodetic observations. The first is participation in JADE (JApanese Dynamic Earth observation by VLBI) organized by GSI (Geographical Survey Institute) and IVS-T2 session in order to link the VERA coordinates to the ITRF2008 (International Terrestrial Reference Frame 2008). Basically Mizusawa station participates in JADE nearly every month. Based on the observations for four years, the 3-dimensional positions and velocities of Mizusawa station till 09/Mar/2011 is determined with accuracies of 7-9 mm and about 1 mm/yr in ITRF2008 coordinate system. But the uncertainty of several centimeters exists in the position on and after March 11, 2011. The second kind of geodetic observations is monitoring of baseline vectors between VERA stations by internal geodetic VLBI observations. Geodetic positions of VERA antennas relative to Mizusawa antenna are measured from geodetic VLBI observations every two weeks. From polygonal fitting of the six-year geodetic results, the relative positions and velocities are obtained at the precisions of 1-2 mm and 0.8-1 mm/yr till 10/Mar/2011. The third kind is continuous GPS observations at the VERA sites for interpolating VLBI geodetic positions. Daily positions can be determined from 24 hour GPS data. The GPS observations are also used to estimate tropospheric zenith delay of each VERA site routinely. The time resolution of delay estimates is 5 minutes.

#### 2.8.2 Brief Summary of KVN Geodetic Measurement

KVN antenna positions are regularly monitored using GPS and geodetic VLBI observations. The K band geodesy VLBI program between KVN and VERA has been started in 2011 (see Table 9). Current KVN antenna positions (see Table 1) are obtained from the KaVA K-band geodesy on January 24, 2014. The typical 1-sigma errors of geodetic solutions are about 0.4 cm in X, Y, and Z directions. Based on 10 epoch KaVA K-band geodetic observations from Sep. 2012 to Nov. 2014, uncertainty of KVN antenna positions are  $\sim 1.39$  cm at Yonsei,  $\sim 1.05$  cm at Ulsan and  $\sim 1.03$  cm at Tamna.

Table 9: The status of KaVA K band geodesy observations.

Table 5. The status of May 11 band geodesy observations.			
Obs. Code	Obs. Date	Antenna	Note
r11333k	2011 Nov. 29	Ky Ku Kt Vm Vr Vs Vo	VERA+Yonsei solution was obtained.
r11361k	2011 Dec. 27	Ky Kt Vm Vr Vs Vo	Observation failed.
r12271k	2012 Sep. 27	Ky Ku Kt Vm Vr Vs Vo	All solutions were obtained.
r13088k	2013 Mar. 29	Ky Ku Kt Vm Vr Vs Vo	All solutions were obtained.
r13140k	$2013~\mathrm{May}~20$	Ky Ku Kt Vm Vr Vs Vo	All solutions were obtained.
r13251k	2013 Sep. 9	Ky Ku Kt Vm Vr Vs Vo	All solutions were obtained.
r13313k	2013 Nov. 9	Ky Ku Kt Vm Vr Vs Vo	Yonsei solution was failed.
r14028k	2014  Jan.  28	Ky Ku Kt Vm Vr Vs Vo	All solutions were obtained.
r14095k	2014 Apr. 5	Ky Ku Kt Vm Vr Vs Vo	All solutions were obtained.
r14159k	2014 Jun. 8	Ky Ku Kt Vm Vr Vs Vo	All solutions were obtained.
r14246k	2014 Sep. 3	Ky Ku Kt Vm Vr Vs Vo	All solutions were obtained.
r14305k	2014 Nov. 1	Ky Ku Kt Vm Vr Vs Vo	All solutions were obtained.
r15027k	$2015~\mathrm{Jan.}~27$	Ky Ku Kt Vm Vr Vs Vo	All solutions were obtained.
r15089k	2015  Mar.  30	Ky Ku Kt Vm Vr Vs Vo	All solutions were obtained.
r15151k	$2015~\mathrm{May}~31$	Ky Ku Kt Vm Vr Vs Vo	All solutions were obtained.
r15242k	2015 Aug. 30	Ky Ku Kt Vm Vr Vs Vo	All solutions were obtained.
r15274k	2015 Oct. 1	Ky Ku Kt Vm Vr Vs Vo	All solutions were obtained.
r15303k	2015 Oct. 30	Ky Ku Kt Vm Vr Vs Vo	Ulsan solution was failed.
r15330k	2015 Nov. 26	Ky Ku Kt Vm Vr Vs Vo	in progress
r15361k	$2015 \ \mathrm{Dec.} \ 27$	Ky Ku Kt Vm Vr Vs Vo	All solutions were obtained.
r16027k	2016 Jan. $27$	Ky Ku Kt Vm Vr Vs Vo	All solutions were obtained.

Ky, Ku, and Kt stand for Yonsei, Ulsan, and Tamna antennas in KVN, respectively.

Vm, Vr, Vs, and Vo represent Mizusawa, Iriki, Ishigakijima, and Ogasawara antennas in VERA, respectively.

# 3 Observing Proposal

### 3.1 Call for Proposal (CfP)

For the KaVA observing season from 15th June 15 2016 to 15th January 2017 (2016B), three 21 m KVN antennas and four 20 m VERA antennas are opened for single-frequency single-polarization (LCP) observations at K and Q bands. Recording rate of 1024 Mbps=1 Gbps (total bandwidth of 256 MHz) will be open for the 2016B CfP. Correlation of the KaVA data will be done by The Daejeon correlator at KJCC. Total observing time up to 250 hours will be available for the common-use observing time for KaVA in the 2016B period. The maximum observing time per proposal is 48 hours. If requested in the proposals, the observation time can be allocated over a year, until January 15, 2017, for this call. But the maximum observation time will be NOT increased. The application must be received by

#### 08:00 UTC on 1st June, 2016

for the 2016B CfP. Proposals from the PIs belonging to any institutes/universities all over the world are also accepted, and proposers are not required to include collaborators from KVN/VERA projects as a co-investigator (CoI). However, PIs are recommended to add at least one collaborator(s) belonging to either KVN or VERA project. Note that the KaVA observing sessions in 2016B will be carried out as risk-shared open use.

### 3.2 Proposal Submission

As for the proposal submission, details and application forms of KaVA proposal can be found at the KaVA CfP web site:

Any questions on proposal submission should be sent to kavaprop (at-mark) kasi.re.kr. We support astronomers in the preparation of proposals, scheduling, and data analysis. For that reason, proposers who are not familiar with KaVA are recommended to include at least one collaborator from VERA or KVN. If it is difficult to find collaborators from VERA or KVN, please consult us to find one. The contact address for the support is kavaprop (at-mark) kasi.re.kr.

Proposals submitted for the 2016B CfP will be reviewed by the referees consisted of KVN and VERA referees already assigned to each array. KaVA makes technical review of all the proposals. The KVN Time Allocation Committee (TAC) and VERA Program Committee (PC) make rating of each KaVA proposal based on the referees, and the KaVA Combined TAC (CTAC) decide the allocation based on each rating result. The results of the review will be announced to PIs in late July.

#### 3.3 Observation Mode

The K band and the Q band single-frequency single-polarization modes are available and a recording rate of 1024 Mbps (total bandwidth of 256 MHz) will be open for the 2016B CfP. Dual-beam mode with VERA and dual-polarization with KVN will not be available for the 2016B CfP. For accurate astrometric observations, many items

(antenna positions, calibrators, schedule, etc.) should be carefully considered and prepared. At present, astrometric VLBI observations with KaVA is not supported in the 2016B CfP. Two new observation modes are available from this call, Fast antenna nodding mode and 1-beam hybrid (KVN multi-freuquency support) mode, as summarized in the appendix.

### 3.4 Target of Opportunity (ToO) observations

Target of Opportunity proposals can be submitted to regular CfP of KaVA. Also, unexpected or urgent ToO can be submitted Director's time at any time. These proposals must include specific triggering criteria to initiate a observation. The ToO is active one year from it is approved. The proposals to Director's time must be submitted by PDF files using e-mail to kavaprop (at-mark) kasi.re.kr.

### 3.5 Angular Resolution and Largest Detectable Angular Scale

The expected angular resolutions for the K band and the Q band are about 1.2 mas and 0.6 mas, respectively. The synthesized beam size strongly depends on UV coverage, and could be higher than the values mentioned above because the baselines projected on UV plane become shorter than the distance between antennas. The beam size can be calculated approximately by the following formula;

$$\theta \sim 2063 \left(\frac{\lambda}{[\text{cm}]}\right) \left(\frac{B}{[\text{km}]}\right)^{-1} [\text{mas}].$$
 (2)

where  $\lambda$  and B are observed wavelength in centimeter and the maximum baseline length in kilometer, respectively.

The minimum detectable angular scale for interferometers can be also expressed by equation (2), where the baseline length B is replaced with the shortest one among the array. Because of the relatively short baselines provided by KVN,  $\sim 300$  km, KaVA is able to detect an extended structure up to 9 mas and 5 mas for the K and Q bands, respectively.

# 3.6 Sensitivity

When a target source is observed, a noise level  $\sigma_{\rm bl}$  for each baseline can be expressed as

$$\sigma_{\rm bl} = \frac{2k}{\eta} \frac{\sqrt{T_{\rm sys,1} T_{\rm sys,2}}}{\sqrt{A_{e1} A_{e2}} \sqrt{2B\tau}} = \frac{1}{\eta} \frac{\sqrt{SEFD_{\rm sys,1} SEFD_{\rm sys,2}}}{\sqrt{2B\tau}},\tag{3}$$

where k is Boltzmann constant,  $\eta$  is quantization efficiency ( $\sim 0.88$ ),  $T_{\rm sys}$  is system noise temperature, SEFD is system equivalent flux density,  $A_e$  is antenna effective aperture area ( $A_e = \pi \eta_A D^2/4$  in which  $A_e$  and D are the aperture efficiency and antenna diameter, respectively), B is the bandwidth, and  $\tau$  is on-source integration time. Note that for an integration time beyond 3 minutes (in the K band), the noise level expected by equation (3) cannot be attained because of the coherence loss due to the atmospheric fluctuation. Thus, for finding fringe within a coherence time, the

integration time  $\tau$  cannot be longer than 3 minutes. For VLBI observations, signal-to-noise ratio (S/N) of at least 5 and usually 7 is generally required for finding fringes.

A resultant image noise level  $\sigma_{\rm im}$  can be expressed as

$$\sigma_{\rm im} = \frac{1}{\sqrt{\Sigma \sigma_{\rm bl}^{-2}}}.$$
 (4)

If the array consists of identical antennas, an image noise levels can be expressed as

$$\sigma_{\rm bl} = \frac{2k}{\eta} \frac{T_{\rm sys}}{A_e \sqrt{N(N-1)B\tau}} = \frac{1}{\eta} \frac{SEFD}{\sqrt{N(N-1)B\tau}},\tag{5}$$

where N is the number of antennas. Using the typical antenna parameters (Table 10), baseline and image sensitivity values of KaVA are calculated as listed in Table 11.

Table 10: Parameters of each antenna.						
KVN			VERA			
Band	Tsys[K]	$\eta_A$	SEFD [Jy]	Tsys[K]	$\eta_A$	SEFD [Jy]
K	100	0.6	1328	120	0.5	2343
Q	150	0.6	1992	250	0.5	4881

Table 11: Sensitivity of each array.

	Baselin	ne sensitivity	Image sensitivity [mJy]			
Band	VERA-VERA	KVN-KVN	VERA-KVN	VERA	KVN	KaVA
K	10.7	6.1	8.1	0.4	0.3	0.2
Q	22.4	9.1	14.3	0.8	0.5	0.3

Sensitivities  $(1\sigma)$  are listed in unit of mJy.

Integration time of 120 seconds and 4 hours are assumed for baseline and image sensitivities, respectively. Total bandwidth of 256 MHz (for continuum emission) is assumed for all the calculations. In the case of narrower bandwidth of 15.625 KHz (for maser emission), sensitivities can be calculated by multiplying a factor of 128.

Figures 9 and 10 show the system noise temperature at Mizusawa and Ulsan, respectively. For Mizusawa, receiver noise temperatures are also plotted.

Note that the receiver temperature of the VERA antenna includes the temperature increase due to the feedome loss and the spill-over effect. In Mizusawa, typical system temperature in the K band is  $T_{\rm sys}=150~{\rm K}$  in fine weather of winter season, but sometimes rises above  $T_{\rm sys}=300~{\rm K}$  in summer season. The system temperature at Iriki station shows a similar tendency to that in Mizusawa. In Ogasawara and Ishigakijima, typical system temperature is similar to that for summer in Mizusawa site, with typical optical depth of  $\tau_0=0.2\sim0.3$ . The typical system temperature in the Q band in Mizusawa is  $T_{\rm sys}=250~{\rm K}$  in fine weather of winter season, and  $T_{\rm sys}=300-400~{\rm K}$  in summer season. The typical system temperature in Ogasawara and Ishigakijima in the Q band is larger than that in Mizusawa also.

The typical system temperature in the K band at all KVN stations is around 100 K in winter season. In summer season, it increases up to  $\sim 300$  K. In the Q band, the typical system temperature is around 150 K in winter season and 250 K in summer season at Yonsei and Tamna. The system temperature of Ulsan in the Q band is about 40 K lower than the other two KVN stations. This is mainly due to the difference in receiver noise temperature (see Table 5).

#### 3.7 Calibrator Information

The NRAO VLBA calibrator survey is very useful to search for a continuum source which can be used as a reference source to carry out the delay, bandpass, and phase calibrations. The source list of this calibrator survey can be found at the following VLBA homepage,

http://www.vlba.nrao.edu/astro/calib/index.shtml.

For delay calibrations and bandpass calibrations, calibrators with 1 Jy or brighter are strongly recommended as listed in the VLBA fringe finder survey:

http://www.aoc.nrao.edu/~analysts/vlba/ffs.html.

Interval of observing calibrator scans must be shorter than 1 hour to track the delay and delay rate in the correlation process.

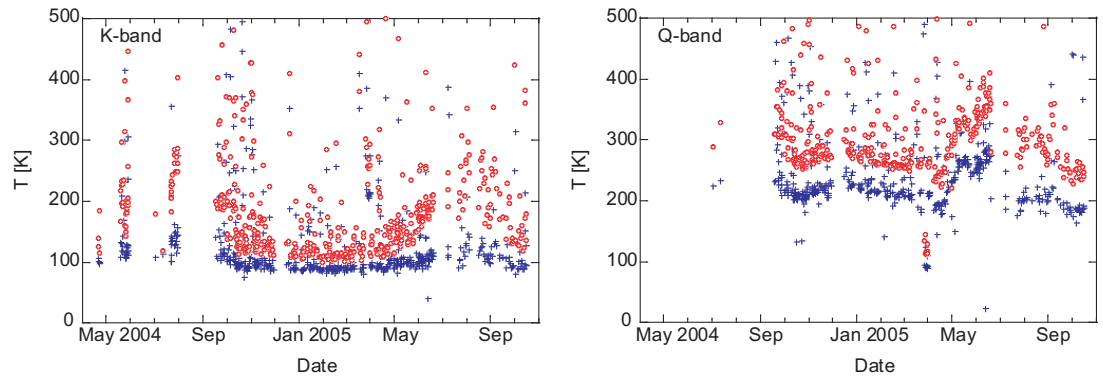


Figure 9: The receiver noise temperature (*blue crosses*) and the system noise temperature (*red open circles*) at the zenith in the K band and the Q band at the Mizusawa station.

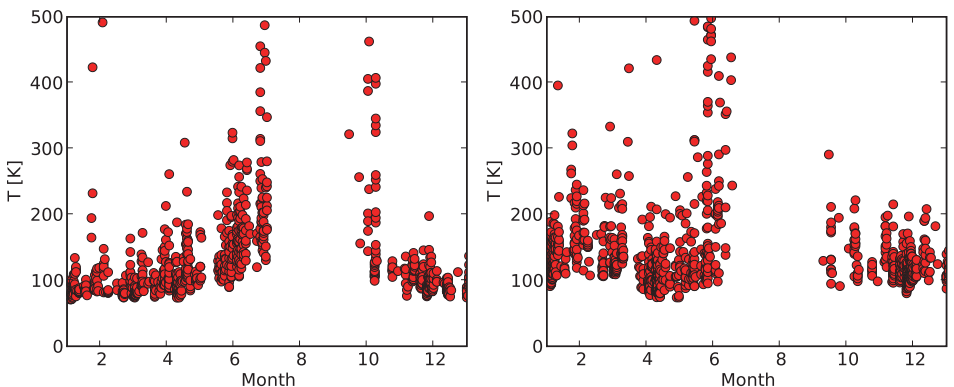


Figure 10: The zenith system noise temperature (red filled circles) at the K band (left) and the Q band (right) in the Ulsan station.

### 3.8 Date Archive

The users who proposed the observations will have an exclusive access the data for 18 months after the correlation. After that period, all the observed data in the KaVA common-use observation will be released as archive data. Thereafter, archived data will be available to any user upon request. This policy is applied to each observation, even if the proposed observation is comprised of multi-epoch observations in this season.

### 4 Observation and Data Reduction

### 4.1 Preparation

After the acceptance of proposals, users are requested to prepare the observing schedule file two weeks before the observation date. The observer is encouraged to consult a contact person in the KaVA AOC members and/or the assigned support scientist to prepare the schedule file under the support of the contact person and/or the assigned support scientist. The schedule submission should be done by a stand-alone vex file. The examples of KaVA vex file are available at the KaVA web site:

http://radio.kasi.re.kr/kava/kava\_observing\_preparation.php

On your schedule, we strongly recommend to include at least two fringe finder scans, each lasting 5 or more minutes at the first and latter part of observation in order to search the delay and rate offsets for the correlation.

We request PIs to specify their correlation parameters at the beginning of the vex file for proper correlation processing. In particular, PIs who request for sub-array or dual-beam observations for KaVA should provide a frequency matching table for the correct correlation.

#### 4.2 Observation and Correlation

KaVA members take full responsibility for observation and correlation process, and thus basically proposers will not be asked to take part in observations or correlations. Observations are proceeded by operators from each side (KVN and VERA) and correlated data is delivered to the users in approximately two months including the time for media shipping to KJCC at Daejeon.

After the correlation, the user will be notified where the data can be downloaded by email. After one month later of a correlated data distribution to PIs, disk modules which contains raw observing data can be recycled without notice. Therefore, PIs should investigate the correlated output carefully. For re-correlation or raw data keeping of the data, PI should provide adequate evidence in order to justify his/her request. If there is an issue related to correlated data, PI should consult a support scientist first or the correlator team (kjcc (at-mark) kasi.re.kr), and not to ask KJCC members directly.

#### 4.3 Data Reduction

For the KaVA data reduction, the users are encouraged to reduce the data using the NRAO AIPS software package. The observation data and calibration data will be provided to the users in a format which AIPS can read.

As for the amplitude calibration, we will provide "ANTAB" files which include the system temperature information measured by the R-sky method and the information of the dependence of aperture efficiency on antenna elevation. If the user wants weather information, the information of the temperature, pressure, and humidity during the observation can be provided.

At present, KaVA does not support for astrometric observations. In case of questions or problems, the users are encouraged to ask the contact person in KaVA members and/or the assigned support scientist for supports.

#### 4.4 Further Information

The users can contact any staff member of the KaVA by E-mail (see Table 12).

Table 12: Contact addresses.

Name	E-mail address	Related Field
Proposal submission	kavaprop (at-mark) kasi.re.kr	Proposal submission in general
User support team	kavahelp (at-mark) kasi.re.kr	User support in general
Operation team	kavaobs (at-mark) kasi.re.kr	Observation related requests/questions schedule submission
Correlator team	kjcc (at-mark) kasi.re.kr	Correlation related requests/questions correlated data distribution

### References

- [1] KaVA web site: http://kava.kasi.re.kr
- [2] KaVA CfP web site: http://veraserver.mtk.nao.ac.jp/restricted/KaVA2016B.html
- [3] VERA web site: http://veraserver.mtk.nao.ac.jp/index.html
- [4] KVN web site: http://kvn-web.kasi.re.kr/eng
- [5] Han et al. 2013, PASP, 125, 539
- [6] Han et al. 2008, Int. J. Infrared Millimeter Waves, 29, 69
- [7] Lee et al. 2011, PASP, 128, 1398
- [8] Matsumoto et al. 2014, ApJL, 789, L1
- [9] Niinuma et al. 2014, PASJ, 66, 103
- [10] Oh et al. 2011, PASJ, 63, 1229

### A New observation mode from 2016B

### A.1 Fast antenna nodding mode

This mode is the conventional mode for VLBI phase reference observations. In this mode, the antenna is nodding between the bright phase calibrator and target source. By fringe fitting of the phase calibrator, the residual phase from the unmodeled clock and atmosphere can be dertermined and then interpolated to the target source to achieve a stable phase of the target source.

With this mode, we can detected and image weak sources, which can not be imaged directly by fringe fitting. This mode will also be used for high accuracy astrometry to derive accurate position, proper motion and parallax of VLBI targets, although we will not guarantee the calibration accuracy for astrometry in the current CfP (2016B).

Right now, for KaVA aray, these are still some limitations of fast antenna nodding mode.

- 1. This mode can only working at K band. Since Q band, with higher frequency then need shorter switch time, which is beyond the ability of VERA antennas. The fastest switching time is 1 min.
- 2. Currently, the KJCC troposphere model (accuracy  $\sim 10$  cm) are not accurate enough for  $\mu$ -arcsecond astrometry. For K band fast antenna nodding mode, the accuracy is  $\sim 3$  mili-arcseconds.

Now, we are keep working to improve KaVA phase-reference and astrometry capabilities: (1) improving accuracy of troposphere and clock model; (2) hybrid phase-reference mode: KVN nodding + VERA two beam staring-mode to achieve a faster nodding speed.

# A.2 1-beam hybrid (K/Q/W) mode

KaVA will enable us to conduct VLBI observations in combinations of different types of antennas (antenna beams), receiving bands, recording rates (namely total band widths), and filtered base band channels in one observing session, whose cross correlation is still valid for the whole or some parts of KaVA. In such "hybrid" observing modes with KaVA, there are some modes that are available in the 2016B CfP described as follows.

Although VERA shall use only one of dual beams in a single frequency band (K or Q), the KVN is able to observe in two to three of K/Q/W bands simultaneously in a common observing session. Please check the KVN status report for W-band information (http://radio.kasi.re.kr/kvn/status\_report\_2016). Signal correlation for all the KaVA baselines is valid for the band in which both the KVN and VERA observe, while that for all the observed bands is valid for the KVN baselines.

Frequency allocations should be made separately to the KVN and VERA, including base band channels that are common between the two arrays in a specific band (K or Q). Note that the number of base band channels or the total bandwidth available per

frequency band is limited, therefore brighter continuum sources should be selected for group-delay calibration.

Moreover, different frequency-band assignment (K or Q) is also available for each of VERA stations to observe in K/Q-bands simultaneously. In this case, it is necessary to confirm that uv-coverages in both bands are suitable for a target source. For example, suppose a simultaneous observation of faint 44 GHz methanol maser and compact 22 GHz water masers. In this case, VERA Iriki station is assigned to a Q-band observation while other VERA stations are assigned to K-band in addition to a simultaneous K/Q-band observation with the KVN. The Q-band array becomes a compact array consisted with KVN three + VERA Iriki stations, while the K-band array becomes an extended array consisted with KVN three + VERA Mizusawa/Ogasawara/Ishigakijima stations.